Cement and Concrete Research 143 (2021) 106393

Contents lists available at ScienceDirect

Cement and Concrete Research

journal homepage: www.elsevier.com/locate/cemconres

Effective cation exchange capacity of calcium silicate hydrates (C-S-H)

Ellina Bernard [a], Yiru Yan [b], Barbara Lothenbach [a,b,*]

[a] University of Bern, Institute of Geological Sciences, Rock-Water Interaction Group, 3012 Bern, Switzerland
[b] Empa, Swiss Federal Laboratories for Materials Science and Technology, Laboratory for Concrete & Construction Chemistry, 8600 Dübendorf, Switzerland

ARTICLE INFO

Keywords:
Calcium silicate hydrate (C-S-H)
Exchange cation capacity (CEC)
Alkali
Cementitious material

ABSTRACT

The binding of alkalis and calcium to calcium silicate hydrate (C-S-H) can be measured by cation exchange using cobalt hexamine solution with adapted pH. The effective cation exchange capacity (CEC) decreased at higher Ca/Si in C-S-H. A maximum of $charge_{exch}$/Si of 0.08–0.10 was measured at Ca/Si = 0.8 decreasing to 0.01–0.02 at Ca/Si = 1.6. At high Ca/Si, only a minor fraction of Ca was present at exchangeable sites, while most of the Ca^{2+} present in interlayer or surface was specifically bound and thus not exchangeable. In contrast, sodium was present only at exchangeable sites in the C-S-H, more at low than at high Ca/Si. An increase of pH in the presence of 100 mmol/L NaOH increased the effective CEC of C-S-H by 5–10% indicating a limited influence of pH on the deprotonation of the silanol groups.

1. Introduction

Calcium silicate hydrate (C-S-H) is the main solid phase present in hydrated Portland cements. The composition of C-S-H may change depending on the availability of calcium and silicon. Hydrated Portland cements usually contain C-S-H with a Ca/Si of ~1.5 to 2 [1]. Cements containing supplementary cementitious materials (SCM) for lowering CO_2 emission of cement industry such as blast furnace slags, fly ash or calcined clays have generally a somewhat lower Ca/Si ratio in C-S-H ≤ 1.6 due to the reaction of the pozzolanic materials with the portlandite. The alkalis contained in Portland cements and SCMs or used as activators sorb partially on C-S-H and remain partially in the pore solution, where they contribute to the high pH values present in the pore solution of Portland cements and blended cements [2,3]. The pH value can strongly affect the stability of the phase assemblage on the cement paste, its integrity and its mechanical properties.

C-S-H has a nano-crystalline structure [4,5], which can be described by a hydrated defective tobermorite structure [5–12], i.e. the silica is arranged in silica chains with a repeating dreierketten structure attached to a calcium oxide sheet. Two silica are connected to the calcium oxide sheet pairing with silica, while the third silica occupies a bridging position and is not directly linked to the calcium sheet. The Ca/Si ratio in tobermorite is 0.83 [13,14], the Ca/Si in C-S-H can vary from 0.7 to 2.0 due to the presence of calcium ions in the interlayer and due to the removal of the bridging silica at higher Ca/Si ratios. At low Ca/Si ratios the bridging silica are present resulting in “infinite” silica chain length as in the tobermorite structure while at high Ca/Si ratios the bridging tetratedral sites are absent and the mean chain length can be reduced to dimer tetratedral sites (=two pairing silica), as detailed in Fig. 1. Calcium ions are present in the interlayer, possibly also substituting some of bridging silicate tetrahedra, particularly at higher Ca/Si as suggested by molecular modelling [8], see Fig. 1. The silica groups in C-S-H are partially deprotonated [15] such that C-S-H has a negative surface charge [16–19], which is compensated by calcium and alkalis ions similarly to clay minerals. Thus three different calcium sites can be distinguished in C-S-H, as visualised in Fig. 1: i) CaO in the main layer, ii) Ca^{2+} in bridging sites, bound directly to the silica chains and iii) hydrated Ca^{2+} ions present in the diffuse layer near the surface or in the interlayer.

Alkalis present in the pore water of cement pastes are partially taken up by C-S-H [10], preferentially at lower Ca/Si ratios and at higher pH values [20–23]. In the presence of high alkali concentrations a shortening of the silica chain length has been observed as well as changes in the basal spacing of C-S-H indicating the uptake of alkalis in the interlayer of C-S-H [22,24,25]. The uptake of alkali at a position near the silica groups is confirmed by the observed shifts of Q^1 Si NMR bands to less negative values indicating an increased presence of alkali ions in the interlayer, which provide a weaker shielding to silicon atoms than calcium ions [22,24,25]. Up to 0.2 Na or K per Si has been observed to be taken up in low Ca/Si C-S-H synthesised in 0.5 M NaOH solution [22]. Different approaches are reported in literature to model the equilibrium between C-S-H and solution as discussed in detail in [10]. This was

* Corresponding author at: University of Bern, Institute of Geological Sciences, Rock-Water Interaction Group, 3012 Bern, Switzerland.
E-mail address: barbara.lothenbach@empa.ch (B. Lothenbach).

https://doi.org/10.1016/j.cemconres.2021.106393
Received 5 October 2020; Received in revised form 21 December 2020; Accepted 6 February 2021
Available online 16 February 2021

achieved successfully with Monte Carlo simulations [17–19], also a few geochemical models are able to describe the incorporation of alkalis in C-S-H [26–28].

This experimental study aims to measure the effective binding of alkalis and calcium to the C-S-H by cation exchange capacity (CEC) measurements. CEC measurements quantify the amount of adsorbed and readily exchangeable cations present in the diffuse layer by its exchange with another, higher charged cation [29]. The understanding of the sorption of alkalis and calcium in the C-S-H structure is decisive for the understanding and modelling of pH values and alkali concentration in hydrating Portland cements and blended cements.

2. Materials and methods

2.1. Synthesis

Calcium oxide and silica fume (SiO_2, Aerosil 200, 0.9 wt% HCl) were used as starting materials for the C-S-H synthesis. CaO was obtained by burning calcium carbonate ($CaCO_3$, Merck, pro analysis) for 2 times 8 h at 900 °C.

To assure a homogeneous suspension a water/solid (W/S) ratio of 20 was chosen. Different amounts of CaO and SiO_2 as described in Table 1 are mixed with MilliQ-water or NaOH solutions (100 mmol/L) in 100 mL containers to obtain C-S-H with different Ca/Si ratios. The containers were sealed and shaken at 100 rpm for 2 months at 20 °C; afterwards the samples were shaken manually once per week. After 7 months, the C-S-H suspensions were separated by water vacuum filtration using nylon filters (0.45 um) under nitrogen gas similar to the procedure outlines in [22]. Directly after filtration, the solids were washed with a 50/50 water-ethanol mix followed by a second washing with ethanol (94 wt% alcohol) to remove dissolved ions and to prevent the precipitation of salts during drying. The samples were freeze dried with liquid nitrogen (at −195 °C) and kept under vacuum for a further 5 days to remove the free water. Finally, the samples were stored in a desiccator with SiO_2 and a saturated solution of KOH to avoid carbonation.

Table 1
Amount of starting materials used for the preparation of the C-S-H.

Name	Targeted molar Ca/Si	SiO_2 (g)	CaO (g)	Solution
C-S-H 0.8	0.8	2.86	2.14	100 mL MilliQ
C-S-H 0.8-0.1	0.8	2.86	2.14	100 mL NaOH solution 100 mmol/L
C-S-H 1.0	1.0	2.58	2.41	100 mL MilliQ
C-S-H 1.0-0.1	1.0	2.58	2.41	100 mL NaOH solution 100 mmol/L
C-S-H 1.2	1.2	2.35	2.64	100 mL MilliQ
C-S-H 1.2-0.1	1.2	2.35	2.64	100 mL NaOH solution 100 mmol/L
C-S-H 1.4	1.4	2.17	2.83	100 mL MilliQ
C-S-H 1.4-0.1	1.4	2.17	2.83	100 mL NaOH solution 100 mmol/L
C-S-H 1.6	1.6	2.00	3.00	100 mL MilliQ
C-S-H 1.6-0.1	1.6	2.00	3.00	100 mL NaOH solution 100 mmol/L

2.2. Analytical techniques

2.2.1. Aqueous phase analysis

The pH values of the solution at equilibrium with the C-S-H samples were measured via a Thermo Scientific™ Orion™ PerpHecT™ ROSS™ Combination pH Micro Electrode in the supernatant of the suspension. The pH values of the CEC solutions (see below) were measured with the same equipment immediately after filtration using standard solution KOH and NaOH for calibration [30]. The concentrations of the dissolved calcium, sodium and potassium in the CEC measurements were quantified using a Dionex DP series ICS-3000 ion chromatography system (IC) with a measurement error $\leq$ 10% in undiluted solutions or in solutions diluted by factors of 10, 100 or 1000.

2.2.2. Solid phase analysis

The dried C-S-H samples were characterised by attenuated total reflectance (ATR) Fourier Transformation-Infrared (FT-IR). The spectra were recorded in the mid-region on a Bruker Tensor 27 FT-IR spectrometer between 600 and 6000 cm^{-1} with a resolution of 6 cm^{-1} by

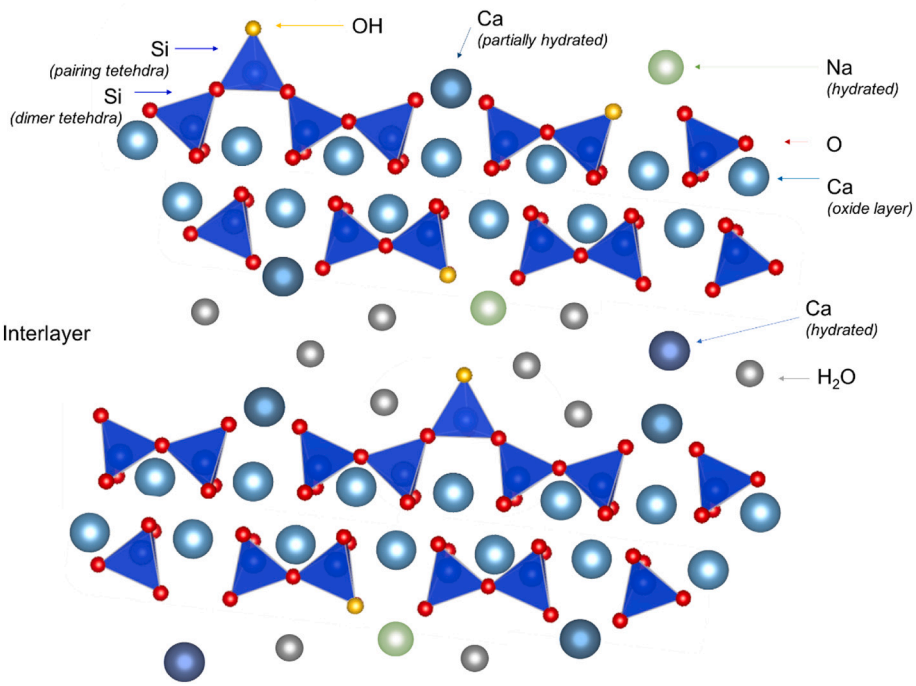

Fig. 1. Schematic sketch of different plausible structure for C-S-H adapted from literature [5–11].

transmittance on small amounts of powder. Spectra were background corrected and scaled to the maximum of Si—O bonds to ease comparison.

2.2.3. Cation exchange capacity

The effective cation exchange capacity (CEC), i.e. the amount of readily exchangeable cations present in the diffuse layer [29], was measured on dried C-S-H powder using 5 mL of cobalt hexamine solution and an equilibration time of 30 min, A method using cobalt hexamine trichloride developed for clay minerals [31] using a concentration of 3 g/L (Sigma-Aldrich, assay: 99%) was chosen because of the high capacity of Co^{3+} to replace bi- and monovalent cations such as Ca^{2+}, $Ca(OH)^{+}$ or Na^{+} on the surface and/or in the interlayer of C-S-H [32]. C-S-H phases, however, can be destabilised at pH below 10. To test whether any dissolution of the C-S-H occurred during the CEC measurements, different time of exposure (30 and 60 min) and different pH values (adapted with NaOH or KOH solution) were investigated.

2.2.3.1. Colorimetry. After the exchange, the suspensions were filtered and the Co^{3+} remaining in solution was measured by colorimetry (absorption band at 473 nm) using a UNI-CAM UV visible spectrometer. The total Co^{3+} adsorbed and thus effective CEC is calculated from the difference in the cobalt hexamine concentration from the original solution (colored) and from the leachate (less colored). In addition, a "total effective CEC" was calculated considering the additional Na and K uptake from the added NaOH/KOH to adapt the pH.

The measured absorbance increased over time in high pH solutions (Fig. 2a), possibly due to the formation of the complex $[Co(H_2O)(OH)]^{2+}$ at high pH [33] or the precipitation of $Co(OH)_3$ or $Co(OH)_2$, which could modify the spectra. Therefore, the colorimetry spectra were measured at the day of the experiment.

Even in short term, the high pH of the solution led to a modification of the absorption spectra of the orange complex formed by the cobalt hexamine as illustrated in Fig. 2a. For the same concentration of cobalt hexamine (i.e. 2.40 ± 0.02 g/L), the absorbance of the whole spectra was higher in 100 mmol/L NaOH than in water. Thus each spectrum was deconvoluted (as shown in Fig. 2b) and the concentration of Co^{3+} was then derived based on the absorbance at 473 nm. With this background correction, the effective Co^{3+} concentration is coherent with the calibration curve recorded at lower pH values over the whole range of Co^{3+} concentrations as shown in Fig. 2c.

2.2.3.2. Released cations. To determine which cations were present on these CEC sites, the concentrations of Na, K and Ca in solution were measured by IC as described in Section 2.2.1. The sorbed K^{+} (in those cases where KOH was used to increase the pH) was obtained from the difference with the K^{+} measured in the initial solution. This concentration was added to the concentration of Co^{3+} sorbed to obtain the

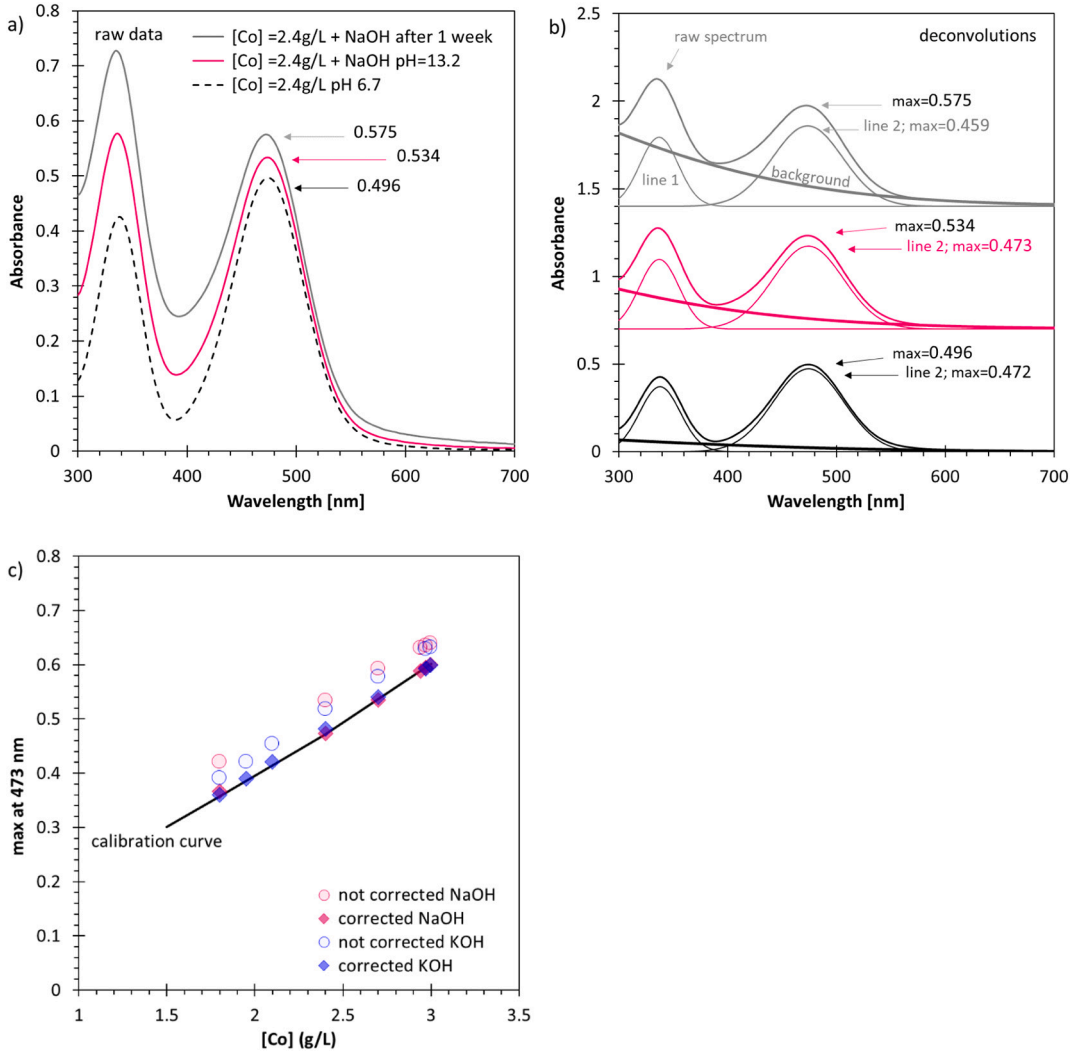

Fig. 2. Effect of pH on the cobaltine hexamine color, a) raw visible spectra depending on the pH and on the age of the solution; b) deconvolutions of the raw spectra; c) not-corrected and corrected absorbance and comparison to the calibration curve measured in solution without NaOH/KOH.

"total effective CEC". The error associated to the total effective CEC is ~15%. The total effective CEC from the Co + K uptake was compared to the sum of released Ca and Na to assess whether dissolution of portlandite and/or a release of Ca due to rearrangement in C-S-H occurred, which would lead to higher released Ca and Na concentrations than total effective CEC.

2.2.4. Total bound Na in C-S-H

The amount of total Na bound in C-S-H was measured by dissolving the 20 mg samples in 10 mL of 0.1 mol/L HCl [22]. Each dissolution was repeated 2 times. Based on the measured Na and Ca concentrations measured by IC, the Na/Ca ratio in C-S-H was calculated.

3. Results and discussions

3.1. Characterisation of C-S-H

The FT-IR spectra of C-S-H are shown in Fig. 3. The characteristic bands of C-S-H centered at ~940–970 cm^{-1} were assigned to Si—O stretching vibrations and those at 800–825 cm^{-1} to Si—O stretching vibrations of Q^1 silica [34]. The FT-IR data indicated the presence of Si—O stretching vibrations in all C-S-H samples, while the Q^1 band became more important with the increase of Ca/Si and the addition of alkalis. This depolymerisation of the silica chains in the C-S-H structures by alkalis agreed with the observations in C-S-H by ^{29}Si MAS NMR [22,24,25]. The signal of the Si—O stretching vibrations at ~940–970 cm^{-1} shifted to lower wavenumbers in the presence of more calcium in the structure, in agreement with Yu et al. [35]. In addition, the presence

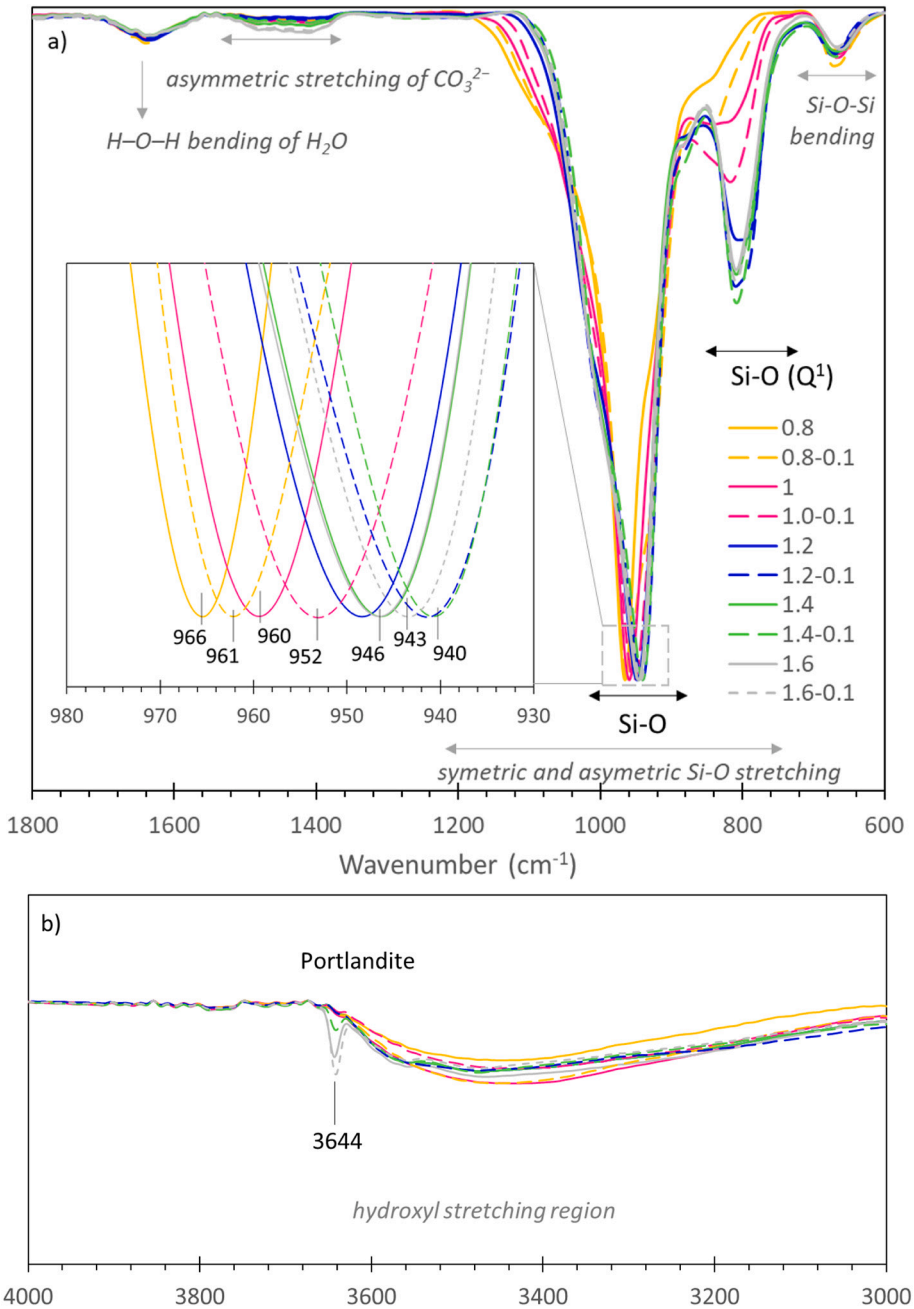

Fig. 3. FTIR spectra of C-S-H samples Ca/Si = 0.8 to 1.4 and C-S-H samples synthesised in NaOH (100 mmol/L) Ca/Si = 0.8 to 1.4. a) Range: 600–1800 cm^{-1}, b) range: 3000–4000 cm^{-1} (hydroxyl stretching region).

of 100 mmol/L NaOH resulted in a shift to lower wavenumbers, indicating a change in the neighbouring cations.

The band corresponding to the asymmetric stretching of CO_3^{2-} was weak indicating that carbonation was limited during the synthesis. Additionally, the band of bending of the water was also very low confirming a similar drying state for all samples. For the samples C-S-H 1.6 and the samples C-S-H 1.4 and 1.6 synthesised in presence of 100 mmol/L NaOH some portlandite was present (band at 3644 cm^{-1} [34]), in agreement with the observations reported in [22].

The pH measurements shown in Table 2 were comparable to the pH measured by L'Hôpital et al. [22] on synthetic C-S-H using the same procedure confirming that equilibrium was reached and that no significant carbonation (<0.5 wt%) had occurred.

3.2. Optimisation of CEC measurement: pH, measurement time and solid to liquid ratio

The measurement of CEC is known to be affected by time (in addition to cations exchanged, the partial dissolution of solid phases may increase the measured CEC with time) as well as by the pH value during the measurements, as a lowering of pH during the measurement could also lower the negative surface charge and thus the CEC as discussed in [36]. Thus, relatively short periods of equilibration times are used to allow the exchange of cations in the diffuse layer, but to prevent the dissolution or restructuring of the solid C-S-H. For clays and magnesium silicate hydrates (M-S-H), contact times of 15 to 30 min are sufficient to obtain a total CEC [37], which captures both the cations in the diffusive layer at the external surface as well those in the interlayer [32,38].

An increase of the duration of the Co sorption from 30 min to 1 h resulted in a slight decrease of the CEC measured by colorimetry of C-S-H and in increase of pH value of the solutions as illustrated in Fig. 4a. This might indicate a rearrangement in the structure of the solid and/or partial dissolution at 1 h, thus all further data refer to the CEC measured after 30 min. A pure solution of Co^{3+} exhibits a pH of ~6.7, which lowers the pH in solution to ~11 compared to the original pH of 12.1 or 12.9 of the solution in which the C-S-H samples were equilibrated for C-S-H 1.0 without and with 0.1 M of NaOH, as illustrated in Fig. 4a. To counteract the strong pH decrease, a Co^{3+} solution doped with NaOH (or KOH) were used to increase the pH to a value more similar to the original solution.

The equilibration of C-S-H with the not-doped Co^{3+} solution decreased the pH of the C-S-H from 12.1 to ~11.2–11.3, while the use of the NaOH-doped Co^{3+} solution increased the final pH to 11.6–11.7. Similar observations were made for a C-S-H synthesised in 100 mmol/L NaOH (initial pH 12.9), where the pH also had to be readjusted in the Co^{3+} solution. The CEC measured based on Co^{3+} sorption after 30 min of equilibration was between 49.8 and 52.8 meq/100 g with no clear trends as a function of pH. This tentatively indicates that the negative charge of the silanol groups in C-S-H does not strongly vary between pH 11.1 to pH 11.7. This weak dependence of effective CEC on pH is consistent with the results of ab initio molecular simulations [15], which have shown that the silanol groups in C-S-H are partially deprotonated at pH 10 and above.

The effective CEC measured based on Co^{3+} sorption on C-S-H 1.0 synthesised in water and in 100 mmol/L NaOH was compared to its effective CEC measured by IC in Fig. 4b to obtain the nature of the exchangeable cations and assess possible dissolution. Fig. 4b shows that the total released cations (as measured by IC) agrees with the measured CEC (based on the Co uptake) only for those samples, which have been measured in Co solutions for 30 min, where the pH has been adapted. In contrast, the samples measured in undoped NaOH-solutions, where the pH was lowered more strongly, showed a clearly higher release of Ca into the solution, indicating a partial dissolution of the C-S-H at lower pH values. The increased dissolution of the C-S-H at lower pH values agrees with observations in literature [39–43].

Table 2
pH measured in the suspension and adapted for 20 °C.

	NaOH (mmol/L)	
	0	100
CSH 0.8	9.8	12.7
CSH 1.0	12.1	12.9
CSH 1.2	12.4	13.1
CSH 1.4	12.7	13.1
CSH 1.6	12.7	13.1

As discussed above, the total released cations measured by IC were in good agreement with the total effective CEC measured by colorimetry, if the pH was maintained, indicating under these conditions (contact time of 30 min and adapted pH) no significant dissolution. The released cations were only Ca^{2+} for the plain C-S-H, while mainly sodium and little calcium was observed for the C-S-H sample prepared in 100 mmol/L NaOH as discussed in more detail in Section 3.4.

In addition to pH and measurement time, also an optimum solid to liquid ratio had to be found to obtain a reasonable decrease of the Co concentrations in the presence of C-S-H, as this depends on the CEC of the solid. Thus different solid to liquid ratios (S/L) of 1/30, 1/80 and 1/250 were investigated. The effective CEC results measured by colorimetry with these three different ratios are shown in Fig. 5. The effective CEC obtained with the highest dilution (S/L = 250) are higher and exhibits a higher error due to the lower amount of solid present and the resulting low difference in the measured Co concentration before and after sorption. In addition, a clear release of Ca was found for these samples indicating an increased dissolution of C-S-H at those very high solid to liquid ratios.

The two lower dilutions (S/L = 30 or 80) showed similar results indicating good conditions for the Co-measurement in both cases. For the lowest dilution (i.e. S/L = 30), the total amount of released cations was lower than the total effective CEC based on the amount of Co taken up. The high amount of C-S-H in solution induces relatively high Ca concentrations in solution, which can lead at high pH values and high Ca/Si to the precipitation of portlandite at high pH and thus to too little released cations measured.

Therefore, an average of the results measured at 1/30 and 1/80 is shown in the following sections as it seems the best compromise allowing good conditions to measure Co uptake and to measure cation release. The integrity of the solids after CEC was re-checked by FTIR (not shown). No significant change in the C-S-H structure nor in portlandite content was found in the solids after the CEC measurement. In a further step, it was found that the use of KOH instead of NaOH to increase the pH of the Co-solution decreased slightly the effective CEC as shown in Fig. 6. However, these differences are within the error of the measurements and thus difficult to interpret. The effective CEC presented below focusses on the CEC measured with KOH doped solution.

To conclude, for optimum CEC measurement of C-S-H samples an intermediate range of liquid to solid ratio between 30 and 80 is recommended as well as an equilibration time of 30 min. In addition, the pH in the CEC solution has to be increased close to the pH value observed in the original equilibrium solution to avoid dissolution and/or re-arrangement in the C-S-H structure.

3.3. CEC of C-S-H without alkalis

The CEC was measured at different targeted Ca/Si from 0.8 and 1.6 in water and NaOH/KOH solutions. The CEC measured at a dilution of 1/80 and 1/30 by colorimetry in NaOH and KOH doped Co-solution give comparable results as discussed above and thus the average is given in Fig. 7a and in Table 3. The effective CEC decreased with the increase of Ca/Si in the C-S-H, indicating a higher ability of C-S-H to bind Ca^{2+} at low Ca/Si ratios, in agreement with the higher sorption of Sr^{2+}, Ra^{2+} or Ba^{2+} measured for low Ca/Si C-S-H [44–47]. The Co^{3+} sorption on C-S-H in water (where up to 20 mmol/L of Ca can be present in solution at Ca/

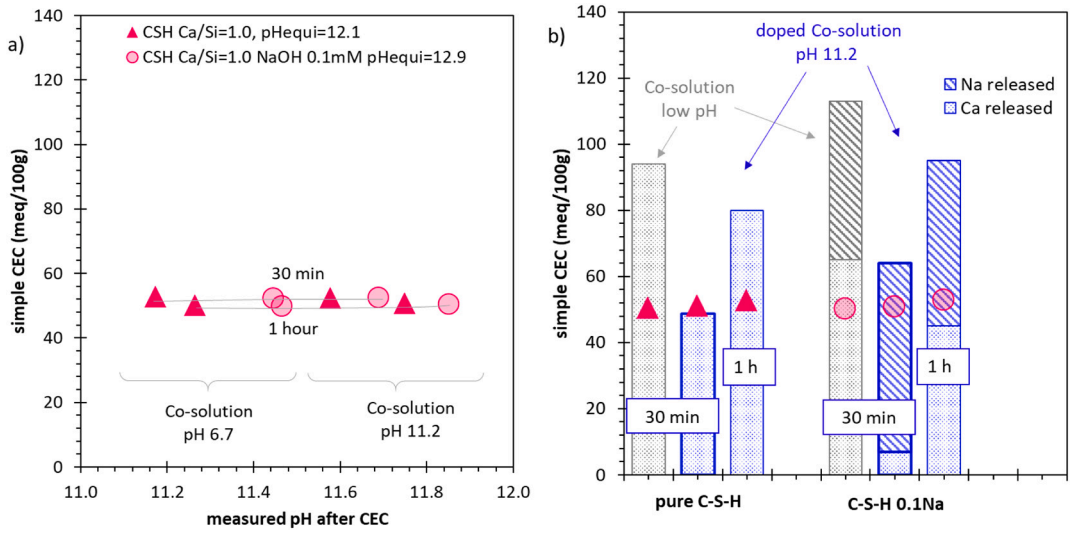

Fig. 4. a) Cation exchange capacity (CEC) measured by cobalt hexamine (circles and triangles) on C-S-H samples with Ca/Si = 1.0 and the effect of increasing the pH during the measurement with 0.1 M NaOH (originally pH 12.9) and of equilibration time; b) comparison between the CEC measured by cobalt hexamine (circles and triangles) and the CEC measured by IC (bars) and cation composition of the CEC measured by IC for the 30 min and 1 h test.

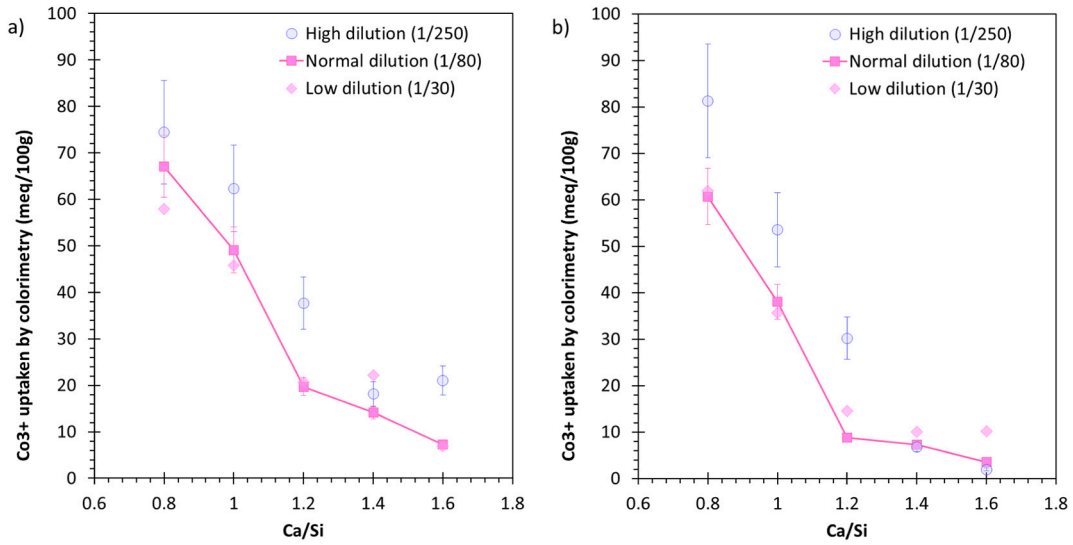

Fig. 5. CEC measured by cobalt hexamine method for the a) pure C-S-H samples and b) C-S-H synthesised in 100 mmol/L NaOH, as a function of initial Ca/Si.

Si = 1.6) is comparable to the sorption in NaOH/KOH solutions (see 3.4.) with ≈1 mmol/L Ca in solution [22], confirming that the used Co^{3+} concentration was sufficient to replace Ca^{2+} also at higher Ca concentrations.

The effective exchangeable calcium was calculated from the average of the CEC (total uptake and total release when dissolution did not occurs) and expressed both per total silicon or per total calcium in C-S-H in Table 3. A CEC of 0.04 Ca^{2+} per silica was observed for C-S-H with Ca/Si = 0.8 indicating the presence of some Ca^{2+} at the surface and the interlayer of C-S-H even at Ca/Si = 0.8. Note that a maximum Ca_{exch}/Si of 0.33 (or CEC = 0.66 eq/Si) could be expected at low Ca/Si if both bridging silanol groups (see Fig. 1) would be deprotonated and their charge only compensated by Ca^{2+}. The considerable lower CEC measured here indicated that a significant part of the silanol groups was protonated in low Ca/Si C-S-H (as suggested by [8] based on molecular simulations) and that these cations were not easily exchangeable but specifically bound. The Ca_{exch}/Si and Ca_{exch}/Ca decrease with the Ca/Si in the C-S-H indicating that a decrease of exchangeable calcium at higher Ca/Si ratio although in total more calcium was present in the C-S-H interlayer and its surface [5,7,8,10,17]. This measured decrease of both the released calcium and the CEC based on Co sorption, indicated thus a specific binding of the calcium present in the C-S-H structure to the silanol groups, and/or that Co^{3+} cannot replace Ca^{2+} present at bridging positions of C-S-H.

3.4. Nature of the CEC in the C-S-H synthesised in the presence of sodium hydroxide/influence of the pH

The results of the CEC measurements for the C-S-H synthesised in presence of NaOH (100 mmol/L) are presented in Fig. 7b and in Table 3. The total CEC as determined by the sorption of Co was comparable or slightly higher to the CEC determined in the C-S-H solutions without alkalis, again indicating that pH had little effect on the measured CEC. As for the samples without alkali, the total CEC decreases with higher Ca/Si in C-S-H underlining the importance of the total Ca-contents in C-S-H on CEC. In the presence of NaOH, the major part of the cations released were Na, indicating a replacement of calcium in the cation exchange sites by sodium. In general, the sorption of bivalent cations

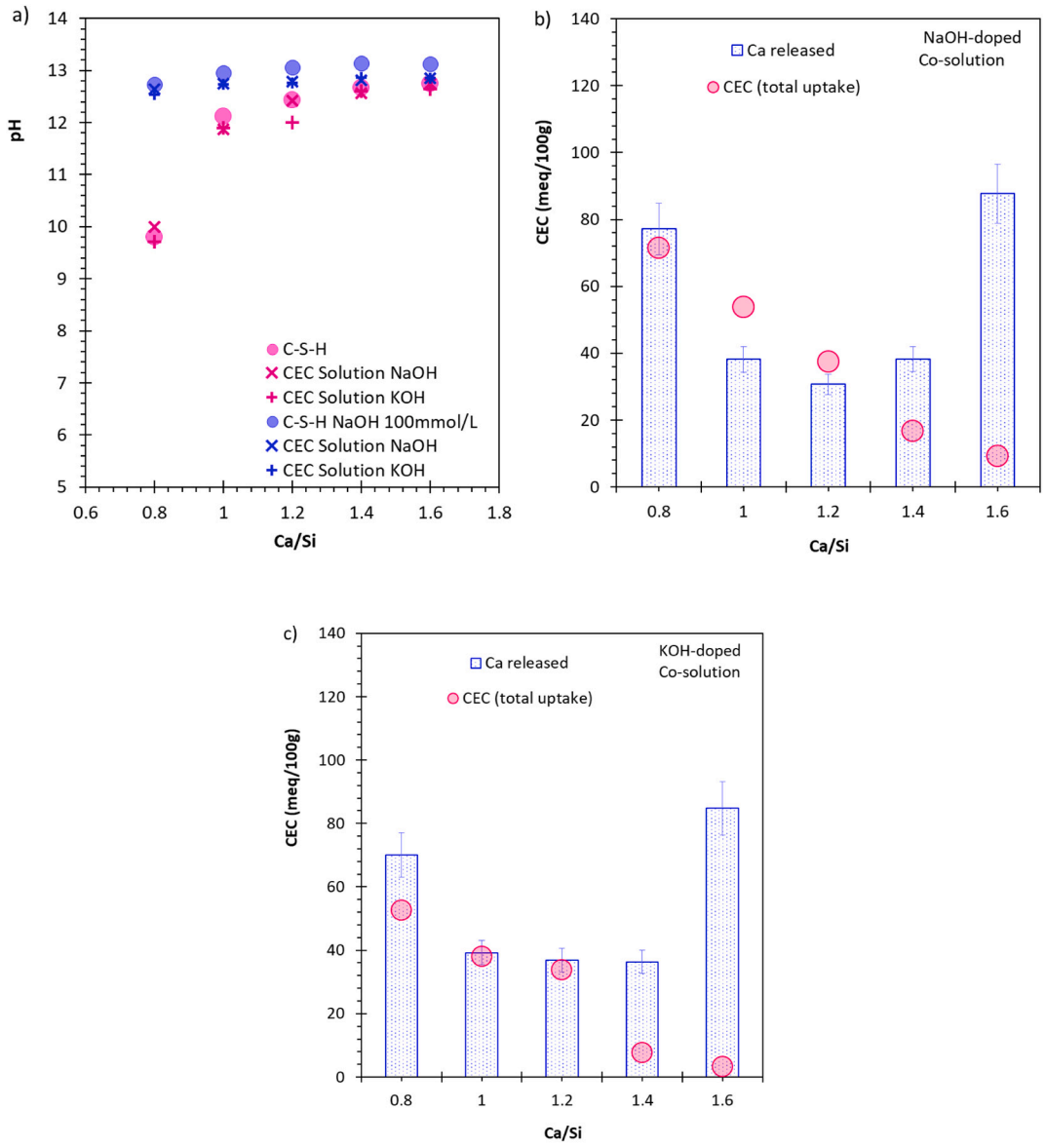

Fig. 6. a) Initial pH and after CEC measurements to ease the comparison, CEC measured for the C-S-H samples measured by cobalt hexamine (dilution 1/80) and taking into account the K taken up as a function of initial Ca/Si, b) pH increased with NaOH; c) pH increased with KOH.

was preferred over monovalent cations [48–50]. However, the much higher Na concentrations (100 mM) in those samples than the 0.01 to 1 mmol/L Ca concentrations [22], resulted in more Na on the CEC sites. In fact, the fraction of Ca on the CEC sites increased with the Ca concentration and reached a maximum at Ca/Si = 1.4 and 1.6, where around 1 mmol/L Ca is present in the original equilibrium solution [22], although at the high Ca/Si, the Ca measurements are also increased by a possible portlandite dissolution.

The exchangeable sodium was calculated from the measured total uptake and expressed both per total silicon or total calcium in C-S-H in Table 3. A CEC of 0.10 Na^+ per silica was observed for C-S-H with Ca/Si = 0.8, which is coherent with literature: Na_{exch}/Si ~0.04 in [21] and ~0.10 in [22] for initial concentration of NaOH at 100 mmol/L. These values compared well with the total amount of Na in C-S-H, as measured by the complete dissolution of the C-S-H in HCl, labelled as Na_{tot}/Si in Table 3. This good agreement between the total Na_{tot}/Si with the exchangeable Na_{exch}/Si indicates that all the Na presents in the C-S-H are easily exchangeable.

If the exchangeable sodium was calculated from the sodium and calcium released, more exchangeable sodium was obtained, than the CEC obtained from the uptake of Co^{3+} and/or K^+. This could be due to i) some dissolution of Ca from C-S-H, even if the elevated pH is expected to reduce dissolution, ii) possible C-S-H rearrangement, and/or iii) the presence of extra sodium, calcium and hydroxyl groups in the diffuse layer (interlayer) of the C-S-H, which are not replaced by Co^{3+} due to the higher ionic strength of the Co^{3+} solution leading to a squeezing of the diffuse layer as discussed in [51,52] for swelling clays.

The average of the effective CEC calculated from uptake and from release was in the presence of NaOH approximately 5–10% higher than the CEC of pure C-S-H samples. This could indicate a moderate increase of depolymerisation of the silicate chains of synthetic C-S-H in the presence of sodium hydroxide, i.e. at higher pH, in agreement with trends observed in zeta potential measurements and predicted by molecular modelling [10,15,17,18,53].

3.5. C-S-H interlayer/surface and implication for the structure

The structure of C-S-H based on the defect tobermorite structure with various Ca/Si and without any charge compensation contains a significant amount of hydroxyl groups (see Fig. 1), corresponding in maximum

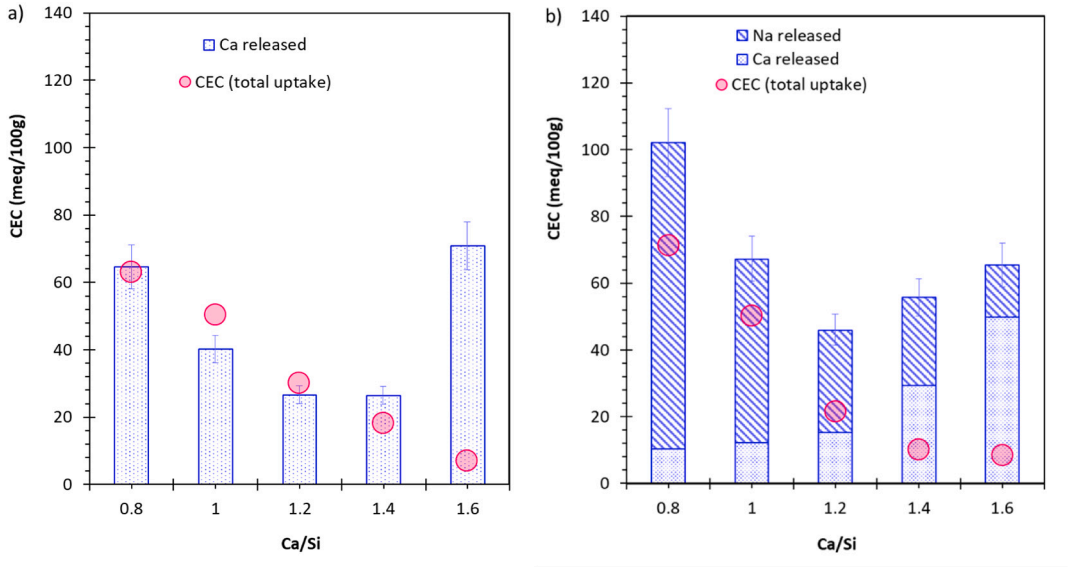

Fig. 7. CEC from the total uptake (Co + K) and the cations released in solution a function of initial Ca/Si; average dilution 1/30 and 1/80, a) pure C-S-H samples and b) C-S-H synthesised in 100 mmol/L NaOH, as a function of initial Ca/Si (values given in Table 3).

Table 3
Average from measurements with the dilution 1/30 and the dilution 1/80: Co and K (used to adapt the pH) taken up and the cations released in solution for the different samples expressed in meq/100g; exchangeable calcium per total silicon or per total calcium for the C-S-H calculated from total uptake (and total release) CEC, error ± 0.01.

C-S-H	Co uptake	K uptake	Total uptake	Ca release	Na release	Total release	lΔl	Ca_{exch}/Si[a]	Ca_{exch}/Ca[a]
0.8	63	1	64	65		65	2	0.041	0.051
1	47	6	53	40		40	7	0.034	0.034
1.2	20	20	40	27		27	6	0.026	0.022
1.4	18	–	18	26		26	8	0.017	0.012
1.6	7	–	7	71		71	64	0.007	0.004

C-S-H 0.1Na	Co uptake	K uptake	Total uptake	Ca release	Na release	Total release	lΔl	Na_{exch}/Si[b]	Na_{exch}/Ca[b]	Na_{exch}/Si[c]	Ca_{exch}/Si[c]	Na_{exch}/Ca[c]	Ca_{exch}/Ca[c]	Na_{tot}/Si[d]
0.8	61	10	71	10	92	102	31	0.096	0.12	0.124	0.005	0.155	0.006	0.096
1	37	13	50	12	55	67	17	0.075	0.075	0.082	0.006	0.082	0.006	0.072
1.2	12	10	22	15	31	46	24	0.035	0.03	0.05	0.008	0.042	0.006	0.06
1.4	9	3	10	30	26	56	46	0.018	0.013	–	–	–	–	0.058[e]
1.6	7	3	8	50	16	65	57	0.016	0.01	–	–	–	–	0.039[e]

[a] Based on the averaged CEC when no dissolution occurred, else, only from the total uptake.
[b] Based on the CEC from the total uptake and considering only Na as exchangeable.
[c] Based on the CEC from the total release.
[d] Total bound Na measured by dissolving 20 mg C-S-H in 10 mL 0.1 M HCl solution.
[e] Dissolution of portlandite is not taken into account.

to two charges per three SiO_2 units at an infinite chain length (low Ca/Si) and to two negative charges per two SiO_2 at high Ca/Si, where only dimers are present. The interlayer of C-S-H and its surface contains cations (H^+, Ca^{2+} or Na^+) contribute to charge balance the negative charge of the deprotonated silanol groups. Labbez et al. [18,54] calculated that approximately 20% of the silanol groups should be deprotonated at pH 10 and above. Similarly, Kuhni Mohamed et al. [8] suggested the presence of mainly protonated silanol groups for low Ca/Si C-S-H, with a schematic structure similar to the one presented in Fig. 1, where O^- of the main layers are compensated by/directly bound to cations. The presence of protonated silanol groups at low Ca/Si is also consistent with the observation of SiO–H stretching signals at low Ca/Si in FTIR studies [35].

The extent of deprotonation depends not only on pH, but also on the kind and concentration of cations present. Calcium ions are strongly attracted by the surface of C-S-H, and the presence of high Ca-concentrations lead to stronger deprotonation of the silanol groups at constant pH than monovalent ions such as K^+ or Na^+ [18]. If C-S-H is more deprotonated, due to higher pH or due to higher Ca^{2+} concentrations at higher Ca/Si ratio, than Ca^{2+} is less and less (energetically and kinetically) easy to desorb which agrees with measurements presented here.

Two types of interlayer calcium can be distinguished: at low Ca/Si, mainly hydrated, easily exchangeable Ca^{2+} is present, which can easily be exchanged by alkalis. This is coherent with literature where alkalis were observed to be better taken up by C-S-H at low Ca/Si [20–23]. At high Ca/Si, the effective CEC results showed that most of the calcium is non-exchangeable, although more total calcium is present in C-S-H. The additional calcium present at high Ca/Si is mainly non-exchangeable, which could correspond to Ca^{2+} present at bridging positions of C-S-H, as suggested based on molecular simulations [8]. These results indicate i) either a specific binding of the Ca^{2+} present in the bridging positions of C-S-H to the pairing silanol groups [8], ii) a higher electrostatic interaction of Ca with the C-S-H surface due to increased

deprotonation of the silonal groups [18] and/or iii) that Co^{3+} cannot replace Ca^{2+} at this position due to steric reasons.

The zeta potential measured in literature [17,18,53] corresponds to the charge of a particle not directly at the surface but in some distance, such that it also could include some interlayer/diffusive layer charges. The zeta potential of C-S-H has been measured to be less negative or even positive if the calcium concentration increases at high Ca/Si ratio, which has been assigned to the presence of specifically bound Ca^{2+} in the Stern layer [17,53]. Thus, an increase of Ca/Si leads to less negative charged surface and to a decrease of CEC, i.e. exchangeable cations positioned in the diffuse layer.

The results of this study are summarised in Fig. 8a to d. At low Ca/Si, cations (Ca^{2+}, Na^{+}) are present in the diffuse layer compensating the negative surface charge of C-S-H and those cations are easily exchangeable. The presence of alkali hydroxide increases the pH and leads to the replacement of Ca^{2+} present in the diffuse layer by Na^{+}. The presence of KOH and NaOH leads also to a somewhat more negative zeta potential [22,55], due to the deprotonation of silanol groups, which results in a moderate increase of the measured CEC (Fig. 7). The presence of NaOH increases in addition the ionic strength, which reduces the double layer thickness around the C-S-H particles.

The presence of mainly non-exchangeable Ca^{2+} at high Ca/Si is in good agreement with the positive zeta potential observed at high Ca/Si [17,53] and the low CEC measured in the present study. As for low Ca/Si C-S-H, the presence of NaOH leads to a replacement of the diffuse layer Ca^{2+} by Na^{+}, while the Ca^{2+} present in the Stern layer is not affected. The capacity of the C-S-H to bind cations depends thus mainly on the Ca/Si in the C-S-H structure and only to a minor extent on the pH.

4. Conclusions

Cation exchange capacity using cobalt hexamine method with adapted pH can measure the effective exchangeable cations in C-S-H. The effective exchangeable cation content of C-S-H decreases with the increase of Ca/Si in the structure. A maximum of $charge_{exch}$/Si of 0.08–0.10 was measured at Ca/Si of 0.8 which decreased to 0.01–0.02 for Ca/Si of 1.6. At high Ca/Si, additional calcium is present as specifically bound Ca^{2+}, probably present as Ca^{2+} in the bridging positions of C-S-H, which cannot by exchanged by Co^{3+}.

The comparison between total dissolution and CEC measurement showed that the sodium in the C-S-H is only exchangeable and that no or only trace sodium is incorporated in the main layer.

An increase of the pH in the presence of 100 mmol/L NaOH solution increases the CEC of C-S-H by approximately 5–10%, in particular at low Ca/Si. This indicates a minor influence of pH in the pH range 10 to 13 on the deprotonation of the silanol groups as the effective CEC does not significantly change.

The CEC method using cobalt hexamine trichloride originally developed for clay minerals [31] could be adapted to C-S-H, by increasing the pH in the measuring solution, to avoid destabilisation of C-S-H at lower pH values. In addition a short exposure time of 30 min and a solid to solution ratio between 30 and 80 gave the best results.

The value of the effective CEC of C-S-H is only weakly influenced by the pH value but strongly decreases due to the presence of specifically bound Ca^{2+} at high Ca/Si. In hydrated Portland cement, where C-S-H shows a Ca/Si ratio of 1.5–2.0, the capacity of C-S-H to bind toxic and/or radioactive cations is therefore expected to be small. In contrast, blended cements containing silica-rich supplementary cementitious materials (SCMs), which results in C-S-H with lower Ca/Si [1], can be

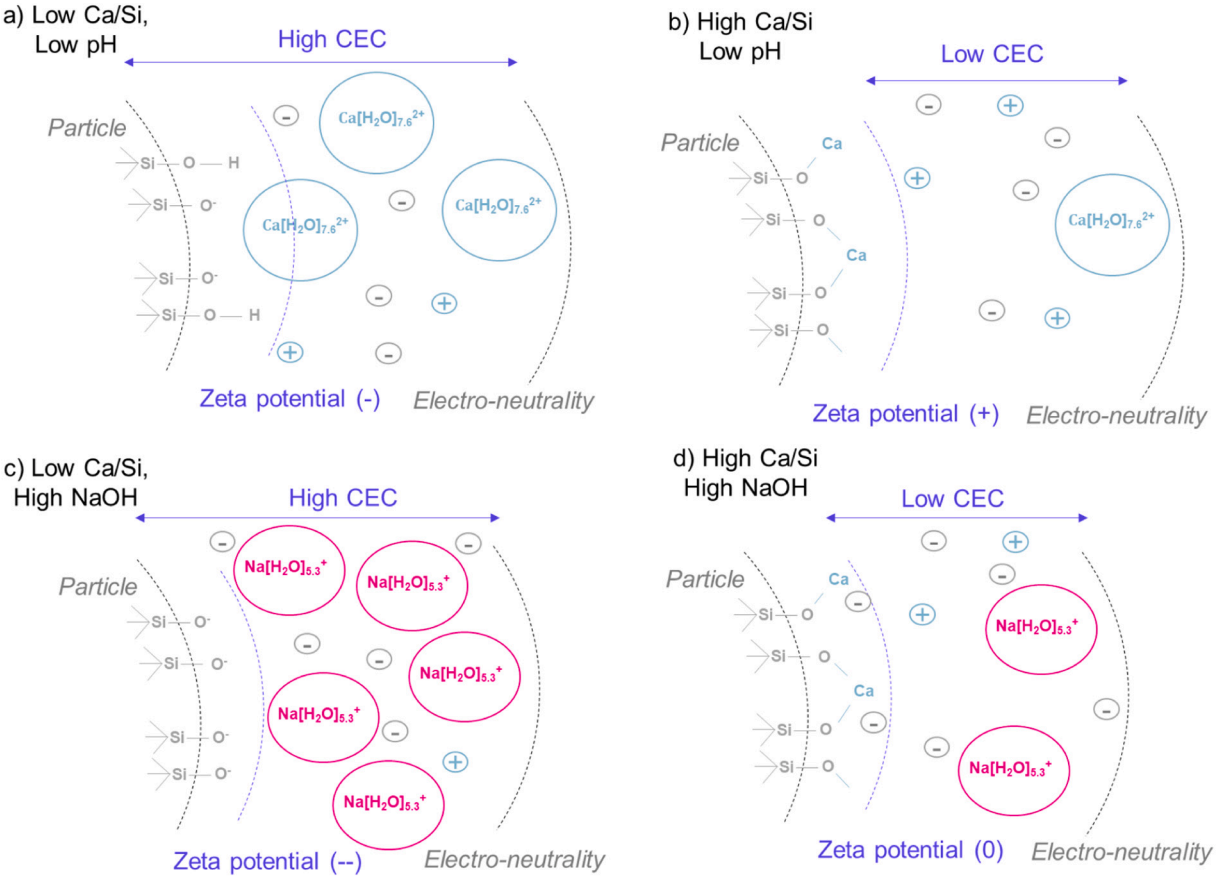

Fig. 8. Schematic sketches of the surface particle of C-S-H based on CEC and Zeta potential measurements; a) low Ca/Si, low pH, b) high Ca/Si, low pH, c) low Ca/Si, high NaOH, d) high Ca/Si, high NaOH.

expected to bind more cations and are thus of interest for the retention of toxic cations and radionuclides. CEC can possibly also be affected by the incorporation of aluminium in C-S-H [56], which is of importance for the understanding and modelling of C-S-H and C-A-S-H and will influence the retention capacity, the transport and durability of blended cements.

CRediT authorship contribution statement

Ellina Bernard: Conceptualization; Methodology; Formal analysis; Investigation; Validation; Writing – original draft
Yiru Yan: Formal analysis; Investigation; Writing – review & editing
Barbara Lothenbach: Supervision; Investigation; Validation; Writing – review & editing.

Declaration of competing interest

The authors declare that they have no known competing financial interests or personal relationships that could have appeared to influence the work reported in this paper.

Acknowledgements

The authors would like to thank Dmitrii Kulik, Christophe Labbez, Dan Miron and Aslam Kunhi Mohamed for helpful discussions. The financial support of the Swiss National Science Foundation (SNSF) project No. 200021_169014 for Y. Yan is gratefully acknowledged.

Appendix A. Supplementary data

Supplementary data to this article can be found online at https://doi.org/10.1016/j.cemconres.2021.106393.

References

[1] B. Lothenbach, K. Scrivener, R. Hooton, Supplementary cementitious materials, Cem. Concr. Res. 41 (2011) 1244–1256.
[2] A. Vollpracht, B. Lothenbach, R. Snellings, J. Haufe, The pore solution of blended cements: a review, Mater. Struct. 49 (2016) 3341–3367.
[3] B. Lothenbach, F. Winnefeld, Thermodynamic modelling of the hydration of Portland cement, Cem. Concr. Res. 36 (2006) 209–226.
[4] A.J. Allen, J.J. Thomas, H.M. Jennings, Composition and density of nanoscale calcium–silicate–hydrate in cement, Nat. Mater. 6 (2007) 311–316.
[5] S. Grangeon, A. Fernandez-Martinez, A. Baronnet, N. Marty, A. Poulain, E. Elkaim, C. Roosz, S. Gaboreau, P. Henocq, F. Claret, Quantitative X-ray pair distribution function analysis of nanocrystalline calcium silicate hydrates: a contribution to the understanding of cement chemistry, J. Appl. Crystallogr. 50 (2017) 14–21.
[6] I.G. Richardson, The calcium silicate hydrates, Cem. Concr. Res. 38 (2008) 137–158.
[7] I.G. Richardson, Model structures for C-(A)-SH (I), Acta Crystallogr. Sect. B: Struct. Sci. Cryst. Eng. Mater. 70 (2014) 903–923.
[8] A.K. Mohamed, S.C. Parker, P. Bowen, S. Galmarini, An atomistic building block description of CSH-towards a realistic CSH model, Cem. Concr. Res. 107 (2018) 221–235.
[9] H.F. Taylor, Proposed structure for calcium silicate hydrate gel, J. Am. Ceram. Soc. 69 (1986) 464–467.
[10] B. Lothenbach, A. Nonat, Calcium silicate hydrates: solid and liquid phase composition, Cem. Concr. Res. 78 (2015) 57–70.
[11] M.R. Andalibi, A. Kumar, B. Srinivasan, P. Bowen, K. Scrivener, C. Ludwig, A. Testino, On the mesoscale mechanism of synthetic calcium–silicate–hydrate precipitation: a population balance modeling approach, J. Mater. Chem. A 6 (2018) 363–373.
[12] A. Kumar, B.J. Walder, A. Kunhi Mohamed, A. Hofstetter, B. Srinivasan, A. J. Rossini, K. Scrivener, L. Emsley, P. Bowen, The atomic-level structure of cementitious calcium silicate hydrate, J. Phys. Chem. C 121 (2017) 17188–17196.
[13] E. Bonaccorsi, S. Merlino, A.R. Kampf, The crystal structure of tobermorite 14 Å (plombierite), a C–S–H phase, J. Am. Ceram. Soc. 88 (2005) 505–512.
[14] S. Merlino, E. Bonaccorsi, T. Armbruster, The real structure of tobermorite 11Å normal and anomalous forms, OD character and polytypic modifications, Eur. J. Mineral. 13 (2001) 577–590.
[15] S.V. Churakov, C. Labbez, L. Pegado, M.L. Sulpizi, Intrinsic acidity of surface sites in calcium-silicate-hydrates and its implication to their electrokinetic properties, J. Phys. Chem. C 118 (2014) 11752–11762.
[16] J. Haas, A. Nonat, From C–S–H to C–A–S–H: experimental study and thermodynamic modelling, Cem. Concr. Res. 68 (2015) 124–138.
[17] C. Labbez, A. Nonat, I. Pochard, B. Jönsson, Experimental and theoretical evidence of overcharging of calcium silicate hydrate, J. Colloid Interface Sci. 309 (2007) 303–307.
[18] C. Labbez, I. Pochard, B. Jönsson, A. Nonat, CSH/solution interface: experimental and Monte Carlo studies, Cem. Concr. Res. 41 (2011) 161–168.
[19] C. Labbez, B. Jönsson, I. Pochard, A. Nonat, B. Cabane, Surface charge density and electrokinetic potential of highly charged minerals: experiments and Monte Carlo simulations on calcium silicate hydrate, J. Phys. Chem. B 110 (2006) 9219–9230.
[20] T. Bach, E. Chabas, I. Pochard, C. Cau Dit Coumes, J. Haas, F. Frizon, A. Nonat, Retention of alkali ions by hydrated low-pH cements: mechanism and Na^+/K^+ selectivity, Cement and Concrete Research, 51 (2013) 14–21.
[21] S.-Y. Hong, F. Glasser, Alkali binding in cement pastes: part I. The CSH phase, Cem. Concr. Res. 29 (1999) 1893–1903.
[22] E. L'Hôpital, B. Lothenbach, K. Scrivener, D. Kulik, Alkali uptake in calcium alumina silicate hydrate (CASH), Cem. Concr. Res. 85 (2016) 122–136.
[23] H. Stade, On the reaction of CSH (di, poly) with alkali hydroxides, Cem. Concr. Res. 19 (1989) 802–810.
[24] R.J. Myers, E. L'Hôpital, J.L. Provis, B. Lothenbach, Effect of temperature and aluminium on calcium (alumino)silicate hydrate chemistry under equilibrium conditions, Cem. Concr. Res. 68 (2015) 83–93.
[25] N. Garg, V.O. Özçelik, J. Skibsted, C.E. White, Nanoscale ordering and depolymerization of calcium silicate hydrates in the presence of alkalis, J. Phys. Chem. C 123 (2019) 24873–24883.
[26] R.J. Myers, S.A. Bernal, J.L. Provis, A thermodynamic model for C-(N-) ASH gel: CNASH_ss. Derivation and validation, Cem. Concr. Res. 66 (2014) 27–47.
[27] B. Lothenbach, G. Le Saout, M. Ben Haha, R. Figi, E. Wieland, Hydration of a low-alkali CEM III/B–SiO2 cement (LAC), Cem. Concr. Res. 42 (2012) 410–423.
[28] D. Kulik, J. Tits, E. Wieland, Aqueous–solid solution model of strontium uptake in C–S–H phases, Geochim. Cosmochim. Acta 71 (2007) A530.
[29] G. Sposito, Surface-reactions in natural aqueous colloidal systems, Chimia 43 (1989) 169–176.
[30] B. Traynor, H. Uvegi, E. Olivetti, B. Lothenbach, R.J. Myers, Methodology for pH measurement in high alkali cementitious systems, Cem. Concr. Res. 135 (2020) 106122.
[31] F. Pearson, D. Arcos, A. Bath, J. Boisson, A.M. Fernández, H. Gäbler, E. Gaucher, A. Gautschi, L. Griffault, P. Hernán, Geochemistry of water in the Opalinus Clay formation at the Mont Terri Rock Laboratory, Report of the Swiss Federal Office for Water and Geology, Geol. Ser. 5 (2003) 319.
[32] E. Bernard, B. Lothenbach, I. Pochard, C. Cau-Dit-Coumes, Alkali binding by magnesium silicate hydrates, J. Am. Ceram. Soc. 102 (2019) 6322–6336.
[33] M.T. Nielsen, K.A. Moltved, K.P. Kepp, Electron transfer of hydrated transition-metal ions and the electronic state of Co3+ (aq), Inorg. Chem. 57 (2018) 7914–7924.
[34] P. Yu, R.J. Kirkpatrick, B. Poe, P.F. McMillan, X. Cong, Structure of calcium silicate hydrate (C-S-H): near-, mid-, and far-infrared spectroscopy, J. Am. Ceram. Soc. 82 (1999) 742–748.
[35] P. Yu, R.J. Kirkpatrick, B. Poe, P.F. McMillan, X. Cong, Structure of calcium silicate hydrate (C-S-H): near-, mid-, and far-infrared spectroscopy, J. Am. Ceram. Soc. 82 (1999) 742–748.
[36] W. Stumm, J.J. Morgan, Aquatic Chemistry. Chemical Equilibria and Rates in Natural Waters, 3rd ed., John Wiley & Sons, Inc., New York, 1996.
[37] A. Jenni, U. Mäder, C. Lerouge, S. Gaboreau, B. Schwyn, In situ interaction between different concretes and Opalinus clay, Phys. Chem. Earth A/B/C 70 (2014) 71–83.
[38] C.A.J. Appelo, D. Postma, Geochemistry, Groundwater and Pollution, CRC Press2004.
[39] E. Bernard, B. Lothenbach, F. Le Goff, I. Pochard, A. Dauzères, Effect of magnesium on calcium silicate hydrate (C-S-H), Cem. Concr. Res. 97 (2017) 61–72.
[40] S.M. Leisinger, A. Bhatnagar, B. Lothenbach, C.A. Johnson, Solubility of chromate in a hydrated OPC, Appl. Geochem. 48 (2014) 132–140.
[41] O. Peyronnard, M. Benzaazoua, D. Blanc, P. Moszkowicz, Study of mineralogy and leaching behavior of stabilized/solidified sludge using differential acid neutralization analysis: part I: experimental study, Cem. Concr. Res. 39 (2009) 600–609.
[42] C. Shi, J. Stegemann, Acid corrosion resistance of different cementing materials, Cem. Concr. Res. 30 (2000) 803–808.
[43] S. Swanton, T. Heath, A. Clacher, Leaching behaviour of low Ca:Si ratio $CaO–SiO_2–H_2O$ systems, Cem. Concr. Res. 88 (2016) 82–95.
[44] J. Tits, K. Iijima, E. Wieland, G. Kamei, The uptake of radium by calcium silicate hydrates and hardened cement paste, Radiochim. Acta 94 (2006) 637–643.
[45] J. Tits, E. Wieland, C. Müller, C. Landesman, M. Bradbury, Strontium binding by calcium silicate hydrates, J. Colloid Interface Sci. 300 (2006) 78–87.
[46] J. Olmeda, T. Missana, F. Grandia, M. Grivé, M. García-Gutiérrez, M. Mingarro, U. Alonso, E. Colàs, P. Henocq, I. Munier, Radium retention by blended cement pastes and pure phases (CSH and CASH gels): experimental assessment and modelling exercises, Appl. Geochem. 105 (2019) 45–54.
[47] T. Missana, M. García-Gutiérrez, M. Mingarro, U. Alonso, Analysis of barium retention mechanisms on calcium silicate hydrate phases, Cem. Concr. Res. 93 (2017) 8–16.
[48] L.S. de Lara, V.A. Rigo, M.F. Michelon, C.O. Metin, Q.P. Nguyen, C.R. Miranda, Molecular dynamics studies of aqueous silica nanoparticle dispersions: salt effects on the double layer formation, J. Phys. Condens. Matter 27 (2015) 325101.
[49] M.C. Bruzzoniti, R.M. De Carlo, S. Fiorilli, B. Onida, C. Sarzanini, Functionalized SBA-15 mesoporous silica in ion chromatography of alkali, alkaline earths, ammonium and transition metal ions, J. Chromatogr. A 1216 (2009) 5540–5547.

[50] J.M. Skluzacek, M.I. Tejedor, M.A. Anderson, An iron-modified silica nanofiltration membrane: effect of solution composition on salt rejection, Microporous Mesoporous Mater. 94 (2006) 288–294.
[51] M. Birgersson, A general framework for ion equilibrium calculations in compacted bentonite, Geochim. Cosmochim. Acta 200 (2017) 186–200.
[52] T. Kozaki, J. Liu, S. Sato, Diffusion mechanism of sodium ions in compacted montmorillonite under different NaCl concentration, Phys. Chem. Earth A/B/C 33 (2008) 957–961.
[53] H. Viallis-Terrisse, A. Nonat, J.-C. Petit, Zeta-potential study of calcium silicate hydrates interacting with alkaline cations, J. Colloid Interface Sci. 244 (2001) 58–65.
[54] I. Pochard, C. Labbez, A. Nonat, H. Vija, B. Jönsson, The effect of polycations on early cement paste, Cem. Concr. Res. 40 (2010) 1488–1494.
[55] S. Barzgar, B. Lothenbach, M. Tarik, A. Di Giacomo, C. Ludwig, The effect of sodium hydroxide on Al uptake by calcium silicate hydrates (CSH), J. Colloid Interface Sci. 572 (2020) 246–256.
[56] G. Sun, J.F. Young, R.J. Kirkpatrick, The role of Al in C–S–H: NMR, XRD, and compositional results for precipitated samples, Cem. Concr. Res. 36 (2006) 18–29.